

Electronic and Photoelectrochemical Properties of Designed Cu(I) Complexes Anchoring with Efficient Donor and Acceptor Units as Sensitizer in DSSC Application

Wichien SANG-AROON^{1,2,*} and Vittaya AMORNKITBAMRUNG^{2,3}

¹Department of Chemistry, Faculty of Engineering, Rajamangala University of Technology Isan, Khon Kaen Campus, Khon Kaen 40000, Thailand

²Integrated Nanotechnology Research Center, Department of Physics, Faculty of Science, Khon Kaen University, Khon Kaen 40002, Thailand

³Thailand Center of Excellence in Physics, CHE, Ministry of Education, Bangkok 10400, Thailand

(*Corresponding author's e-mail: wichien.sa@rmuti.ac.th)

Received: 31 October 2016, Revised: 13 January 2017, Accepted: 20 February 2017

Abstract

In this work, we report the photoelectrochemical properties of 5 designed Cu(I) dyes by means of theoretical approach. The optimized geometries, molecular orbitals electron density and their energy level obtained from DFT/M06/LANL2DZ + DZVP method. The parameters relates to photoelectrochemical properties of these dyes were derived from orbital energy. For all complexes, molecular orbital energy levels meet the requirements for use as sensitizer in DSSC. Introducing the selected ligands has great effect to the MO energies as well as other properties. The quinoxaline-2,3-dithiolate (**1,2**) is great as donor unit but their electrophilic indices indicate that they have less strength of being oxidized confirmed by $E_{OX}^{dye^*}$ and ΔG_{inject} . So, dyes **1** and **2** are not properly suitable for using as sensitizer in DSSC. Surprisingly, hydroxamate ligand shows great potential acceptor unit for Cu(I) in either bipyridine or terpyridine complexes (dyes **3-5**). These dyes present good computed photochemical properties. Thus, the designed dyes **3-5** studied in this work would be competent to provide promising sensitizers for photovoltaic application. Dye **3** is the most efficient, indicating that increasing chromophoric groups or conjugated bridges does not favor to E_{H-L} , eV_{OC} and LHE regards to **4** and **5**.

Keywords: Cu(I) complexes, hydroxamate, quinoxaline-2,3-dithiolate, DSSC, DFT/TDDFT

Introduction

The driving of the development of efficient solar energy conversion system as green energy photovoltaic device depends on the energy crisis, global warming and especially the depletion of fossil fuels. Since discovered by Grätzel and co-workers [1], many researchers have intensified dye-sensitized solar cell (DSSC) as a new promising photovoltaic technology for decade years [2-9]. This kind of solar cell is very attractive because of the possibility of providing a clean and abundant energy source and the large scale production cost would be expected to be lower than that of the conventional silicon solar cell [10-12]. Improvement the performance of photosensitizing components in DSSCs including, semiconductor, dye-sensitizer, electrolyte and electrode systems has been investigated extensively. According to the dye-sensitizer, the best efficient dye is still commonly ruthenium (II) complex compounds [13]. However, searching and improving an inexpensive, more abundant and efficient dyes for DSSC application without depending on a scant resources [14,15] are very timely.

Copper(I) complex compounds possess a wide variety of excited states and also photophysical and photochemical processes. Alonso-Vante *et al.* [16] found that Cu(I) complexes possess similar photo-

physical properties to Ru complexes. This indicates that the repetitious chemical optimization of common metal complexes sensitizers can be comparable to that of Ru complexes [17]. Even though there are some very promising studies by means of both experimental and computational approaches have been reported [18-30] but Cu(I) dyes still have less extensively studied regards to Ru(II) complexes. A recent development by the constable group has been in situ synthesis of heteroleptic Cu(I) dyes on the TiO₂ surface [31]. A 4,4-bis(2-thienyl-5-carboxylic acid) functionalised 2,2-bipyridine ligand and corresponding copper(I) complex was applied in DSSC [32]. It was found that the positioning of the thiophene groups appeared favourable from DFT analysis and the best efficiency of 1.41 % was obtained. Functionalisation of a non-anchoring bipy ligand with a heteroaromatic or a bulky diphenylamino substituent was produced impressive DSSC performances which the best efficiency of 3.8 % has been reported [28]. A new redox couple, [Cu(bpye)₂]⁺²⁺ has been synthesized and utilized in DSSC. Overall efficiencies of 9.0 % at 1 sun and 9.9 % at 0.5 sun were obtained which are considerably higher than those obtained for cells containing the reference redox couple, [Co(bpy)₃]^{2+/3+} [33].

Recently, some computational studies on Cu(I) bipyridyl complexes open the possibility of computationally screening and the way to an effective molecular engineering for further enhance sensitizer [22,31,34-37]. Photophysical properties of Cu(I) complexes containing pyrazine-fused phenanthroline ligands have also been observed by both experimental and theoretical approaches [37]. Nevertheless, these sensitizers might be good sensitizer if they are improved to meet requirements for next generation of DSSC devices. As literature reviewed, both donor and acceptor units in the dye complex systems are improved by experimental and theoretical approaches. A square-planar platinum(II) based dye containing 4,4'-dicarboxy-2,2'-bipyridine and quinoxaline-2,3-dithiolate ligands achieves efficient sensitization of DSSC over a wide visible range, with a solar energy conversion efficiency of 2.6 % [38,39]. This indicates that the dithiolate ligand acts as efficient donor unit in this dye. Conversely, interesting acceptor ligand; hydroxamate exhibits significant efficiency in [Ru(terpy)(tbbpy)L][BF₄]₂ (terpy = 2,2':6',2''-terpyridine, tbbpy = 4,4'-di-tert-butyl-2,2'-bipyridine, L =anchoring ligand) among carboxylate and phosphonate linkers [40]. There have no evidence that either dithiolate donor or hydroxamate acceptor ligands are incooperated into Cu(I) dye complex.

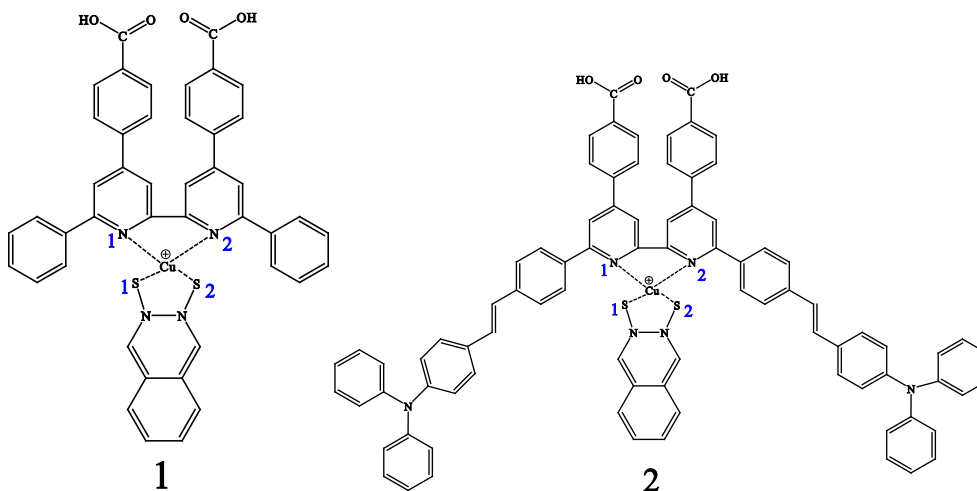


Figure 1 Molecular structure of the designed Cu(I) dyes **1** and **2**.

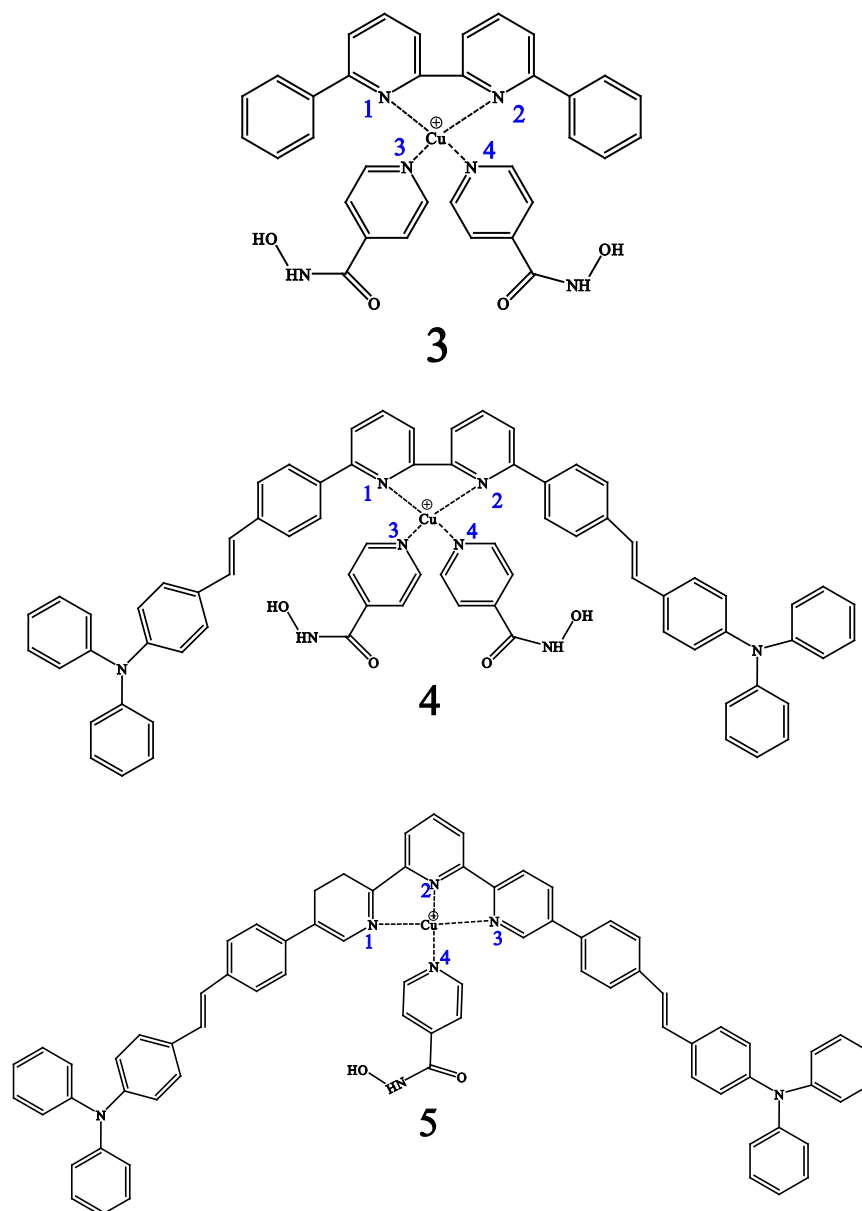


Figure 2 Molecular structure of the designed Cu(I) dyes modeled Cu(I) dyes 3–5.

In the present work, we calculated from theoretical point of view the geometric and spectroscopic properties of 5 $[\text{CuLX}_y]^+$ molecular system. As shown **Figure 1**, L is bipyridyl or terpyridyl ligand, X is quinoxaline–2,3–dithiolate or hydroxamate ligand, y is a number of ligand X in the compounds. In compound **1**, bp conjugates with $-\text{PhCOOH}$ as conjugate bridge and anchoring unit. The $-\text{CH}=\text{CH}-\text{NPh}_3$ moiety ($-\text{NPh}_3$ for short) act as donor unit in **2** by substitution to one of phenyl ring of bipyridyl ligand, pyridine unit also conjugates with $-\text{PhCOOH}$. The quinoxaline–2,3–dithiolate acts as major donor unit in **1** and **2**. On the other hand, in compounds **3–5**, bipyridyl, bipyridyl($-\text{NPh}_3$) and terpyridyl($-\text{NPh}_3$) play as donor unit while hydroxamate performs as acceptor unit display in **Figure 2**.

The aim of this work is to provide a detailed analysis of geometrical and electronic properties of the newly modeled Cu(I) compounds. The spectroscopic as well as photoelectrochemical properties relate to sensitization of the dyes in DSSC are computed based on the DFT and TDDFT method.

Materials and methods

Calculations of the geometrical structures were performed with the Gaussian 09 program [41]. The geometry optimization process was carried out using the density functional theory (DFT) [42-44] with LANL2DZ for C, H, O, N, S atoms [45] and DZVP for Cu atom [46] basis sets, in addition to the hybrid-meta-GGA functional M06 method [47]. The M06 methodology is well-known due to the feasibility for the study of organometallic compounds. The choices of method and basis sets used in this work are referred to the previous work which M06/LANL2DZ+DZVP represents excellent approximations for ionization potential, electron affinity and also maximum absorption wavelength for the Cu(I) biquinoline dyes [36]. The vertical excitation energy and ultraviolet-visible spectra (UV-vis) were simulated by time-dependent DFT (TDDFT) at the same level. The effects of a solvated environment were evaluated with the integral equation formalism polarizable continuum model (IEF-PCM) and the implementation of the non-equilibrium solvation model [48].

The charge transfer properties were analyzed by the free energy change for electron injection (ΔG_{inject}) from excited state dyes to conduction band of TiO_2 [49-51] as Eq. (1);

$$\Delta G_{inject} = E_{OX}^{dye*} - E_{CB}^{TiO_2} \quad (1)$$

$$E_{OX}^{dye*} = E_{OX}^{dye} - E_{00} - \omega_r \quad (2)$$

E_{OX}^{dye*} and E_{OX}^{dye} in Eq. (2) are the excited and ground state oxidation potentials, respectively. E_{OX}^{dye} is computed based on the Rehm and Weller equation as in Eq. (2) [52]. E_{00} is adiabatic energy difference between excited and ground states. The later term can be negligible as mentioned in the previous report [53]. $E_{CB}^{TiO_2}$ corresponds to the conduction band energy level of the TiO_2 semiconductor. $E_{CB}^{TiO_2} = -4.0$ eV [54] obtained from experiment was used because of the value has been observed in the condition which the semiconductor is in contact with aqueous redox solution at fixed pH [55]. Redox potential, $I/I_3^- = -4.8$ eV was used in this work [56].

DFT calculation can possibly find the chemical reactivity descriptors values including chemical hardness (η), chemical potential (μ), electronegativity (χ) and electrophilic index (ω). These descriptors were derived from the first ionization potential (I) and the electron affinity (A) of the N-electron molecular system with a total energy (E) and external potential ($v(\vec{r})$) using the relations as follows [57];

$$\begin{aligned} \chi &\cong -1/2(I + A), \quad \eta = -\chi, \\ -\eta &\cong 1/2(I - A), \\ \omega &\cong \mu^2 / 2\eta, \end{aligned}$$

where $I = -E_{HOMO}$ and $A = -E_{LUMO}$ based on the Koopman theorem [55]. The photovoltaic parameter, open-circuit voltage; eV_{OC} can be estimated theoretically as the difference between E_{LUMO} and $E_{CB}^{TiO_2}$ [49,50,58];

$$eV_{OC} = E_{LUMO} - E_{CB}^{TiO_2} \quad (3)$$

Efficiency of DSSC is related to the dye in response to the incident light. Light harvesting efficiency (*LHE*) is one important factor of the dye. This *LHE* was evaluated by absorption energy of the dye. The *LHE* can be expressed as follows $E_{CB}^{TiO_2}$ [49,50,58];

$$LHE = 1 - 10^{-A} = 1 - 10^{-f} \quad (4)$$

where *A* and *f* are the absorption and oscillating strength, respectively.

Results and discussion

The M06/LANL2DZ + DZVP-optimized structure and selected Cu–N and Cu–S bond lengths of all Cu(I) dyes are displayed in **Figure 3**. It is noted that the total molecular charge of **1** and **2** is –1 where the total charge of **3–5** is +1. Based on the computed bond lengths, it is important to note that the presence of –NPh₃ unit on **2** do not significantly alter the bond length between metal center and bipyridine ligand (Cu–N₁ and Cu–N₂bonds), and those between the metal and quinoxaline–2,3–dithiolate (Cu–S₁ and Cu–S₂ bonds) compare to **1**. When ligand alters from quinoxaline–2,3–dithiolate donor ligand in **1** and **2** to hydroxamate acceptor ligand in compounds **3** and **4**, similar result is found even the –PhCOOH group is not presented. In case of **5**, the Cu–N₄ which corresponds to the bond between metal and hydroxamate ligand is a bit shorter than those of the similar bond (Cu–N₃ and Cu–N₄) in **3** and **4**. The shortest Cu–N bond length is found in Cu–N₄ bond of **5** which is the bond forms between copper and hydroxamate. For **1** and **3**, the replacement of hydroxamate led the Cu–N₁ and Cu–N₂ bonds become longer with respect to quinoxaline–2,3–dithiolate. The theoretical study on copper complexes has previously reported [21,34–37,58]. The bond lengths between Cu and N of bipyridine in our work seem to be longer than those of found in the previous work. It may due to the co-complexation with different ligand and also substituents on the pyridine ring. However, those previous works summarized that M06 functional is more suitable for calculation due to lower error [36]. Based on the structures of the proposed dyes **3–5**, in the case of Ru(II) this ligand is suitable and work nice even in the presence of water [40]. However, one can suspect that this might be difficult in the case of Cu(I). As described above, the bond distances between Cu and N of hydroxamate (Cu–N₁ and Cu–N₂) are shorten than those of Cu and N of bipyridine and terpyridine (Cu–N₃ and Cu–N₄), especially in **5**. This confirms that interaction between Cu and N of hydroxamate are stronger than those of between Cu and N of bipyridine and terpyridine. Thus, it can support the reason that dyes **3–5** incorporating the hydroxamate ligand may be synthetically prepared and structurally stable.

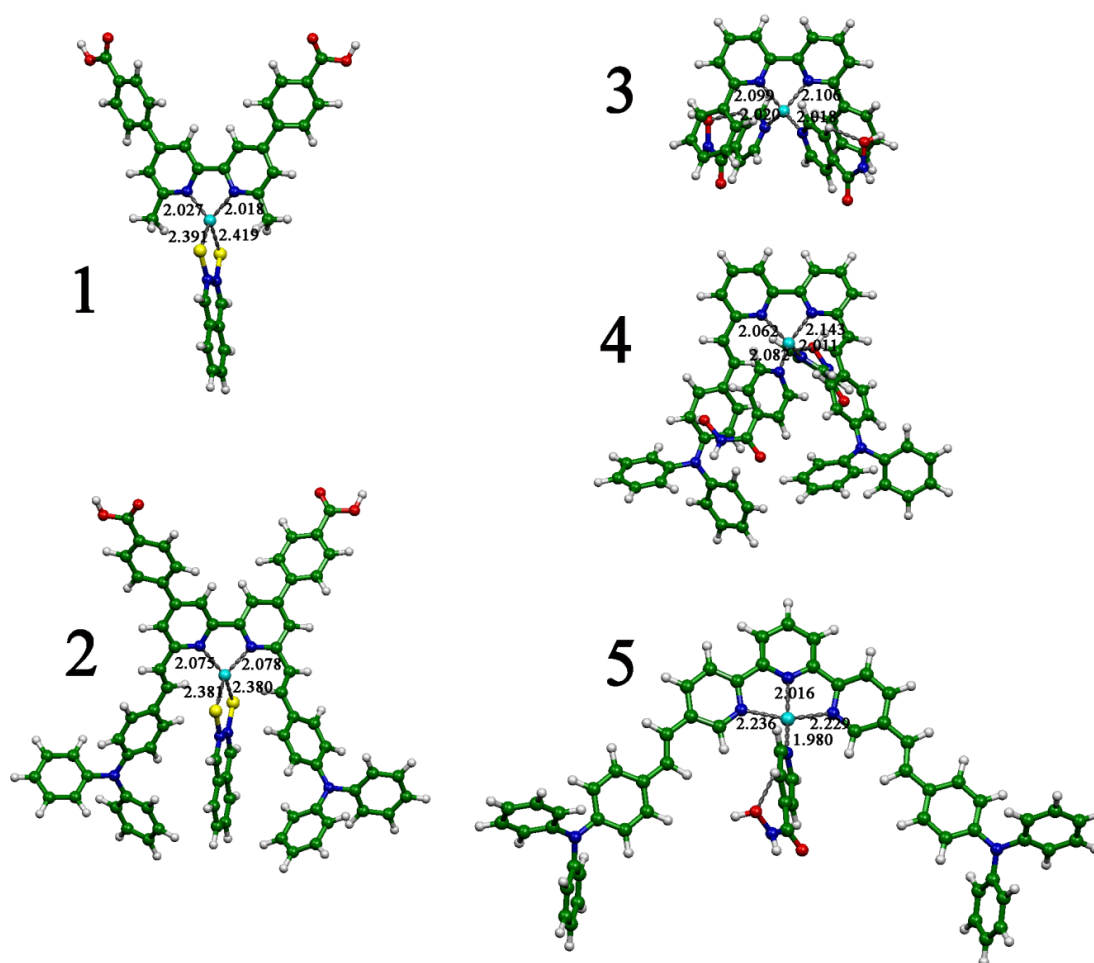


Figure 3 Optimized ground state geometrical structure of Cu(I) dyes 1–5. Bond lengths are in Å

The highest occupied molecular orbital (E_{HOMO}), lowest unoccupied molecular orbital (E_{LUMO}) and energy gap ($E_{\text{H-L}}$) of all dyes computed in 2 different polar media (H_2O and CH_2Cl_2) are tabulated in **Table 1**. E_{HOMO} and E_{LUMO} of dyes 1–5 are down shifted from H_2O to CH_2Cl_2 . It can be observed that addition π -conjugate $-\text{NPh}_3$ on either bipyridine or terpyridine moieties (ligand1) in 2,4 and 5 raises E_{HOMO} in comparison to 1 and 3. For quinoxaline–2,3–dithiolate complexes, the change of bipyridine in 1 to a substituted $-\text{NPh}_3$ bipyridine in 2 does not affect to E_{LUMO} . However, E_{HOMO} of 2 is higher than those of 1 both 2 media. Similarly, for hydroxamate complexes, both E_{HOMO} and E_{LUMO} of these dyes are sequentially up shifted when the ligand change from bipyridine (3) to a substituted $-\text{NPh}_3$ bipyridine (4) and a substituted $-\text{NPh}_3$ terpyridine (5), respectively. Most of the dyes have lower energy gap ($E_{\text{H-L}}$) when the medium changes from polar to non-polar solvent. The $E_{\text{H-L}}$ of all dyes computed in the 2 media are in increasing order: $2 < 1 < 5 < 4 < 3$.

The chemical indices; chemical hardness, chemical potential and Mulliken electronegativity derived from orbital energies of all dyes are listed in **Table 2**. The relative stabilities and chemical hardness of all isomers of dyes based on their frontier molecular orbital energy gap are in the same order and, are in increasing order: $2 < 1 < 5 < 4 < 3$. Thus, it can be interpreted that 3 shows the greatest resistance to change the number of electrons in its systems follow by 4 and 5, respectively. Dyes 1 and 2 have the most

and the second highest Mulliken electronegativity which is higher than the other by 0.517 - 0.667 and 0.517 - 0.708 eV in water and 0.299 - 0.449 and 0.286 - 0.477 eV in CH₂Cl₂. In term of electrophilicity, the result is in contrast to the chemical hardness. The trend of electrophilicity of dyes is in decreasing order: **2** > **1** > **5** > **4** > **3**. Dyes **2** and **1** reveal the greater charge regeneration ability among the others. As observed, the value of all parameters computed in H₂O is lower than those the CH₂Cl₂ except for chemical hardness. This means that these dyes exhibit lower resistance to change the number of electron when dissolving in non-polar solvent. Thus, the greater intermolecular charge transfer of these dyes will be possibly occurred in non-polar solvent. It is important to note that all chemical indices are adjusted based on the neutral species of the dyes. However, these results are important because they can be considered during synthesis to determine the solubility and chemical reactivity of the molecule [36], additionally they can also be employed in photovoltaics, as reported in previous studies [59-61].

Table 1 The highest occupied molecular orbital energy (E_{HOMO}), the lowest unoccupied molecular orbital energy (E_{LUMO}), and HOMO–LUMO energy gap ($E_{\text{HOMO-LUMO}}$) of studied dyes computed at the M06/LANL2DZ+DZVP level of theory.

Dye	E_{HOMO}^a		E_{LUMO}^a		$E_{\text{H-L}}^a$	
	H ₂ O	CH ₂ Cl ₂	H ₂ O	CH ₂ Cl ₂	H ₂ O	CH ₂ Cl ₂
1	-5.796	-6.013	-2.884	-3.156	2.911	2.857
2	-5.360	-5.551	-2.884	-3.156	2.476	2.394
3	-5.632	-5.877	-2.014	-2.258	3.619	3.619
4	-5.306	-5.469	-2.041	-2.286	3.265	3.184
5	-5.224	-5.442	-2.177	-2.394	3.048	3.048

Table 2 Chemical indices of all dyes computed at the M06/LANL2DZ+DZVP level of theory.

Dye	η^a		μ^b		χ^c		ω^d	
	H ₂ O	CH ₂ Cl ₂	H ₂ O	CH ₂ Cl ₂	H ₂ O	CH ₂ Cl ₂	H ₂ O	CH ₂ Cl ₂
1	1.456	1.429	-4.340	-4.585	4.340	4.585	6.468	7.356
2	1.238	1.197	-4.122	-4.354	4.122	4.354	6.862	7.919
3	1.809	1.809	-3.823	-4.068	3.823	4.068	4.040	4.574
4	1.633	1.592	-3.673	-3.877	3.673	3.877	4.131	4.721
5	1.524	1.524	-3.701	-3.918	3.701	3.918	4.494	5.036

^aChemical hardness, $\eta = \Delta E_{\text{HOMO-LUMO}}/2$

^bElectronic chemical potential, $\mu = (E_{\text{HOMO}}+E_{\text{LUMO}})/2$

^cThe Mulliken electronegativity, $\chi = -(E_{\text{HOMO}}+E_{\text{LUMO}})/2$

^dThe electrophilic index, $\omega \cong \mu^2 / 2\eta$

Table 3 The vertical excitation energies, oscillating strengths (f) and transition characters and maximum absorption wavelength (λ_{\max}) of all dyes computed at the TD/M06/LANL2DZ+DZVP of theory.

Dye	Energy ^a		f		Transition character ^{b,c}		λ_{\max} ^a	
	H ₂ O	CH ₂ Cl ₂	H ₂ O	CH ₂ Cl ₂	H ₂ O	CH ₂ Cl ₂	H ₂ O	CH ₂ Cl ₂
1	1.855	1.806	0.021	0.021	H→L (92%)	H→L (92%)	484.5	681.4
	2.328	2.277	0.009	0.010	H-1→L (89%)	H-1→L (89%)		
	2.560	2.529	0.166	0.012	H→L+2 (74%)	H-1→L+1 (72%)		
2	1.832	1.679	0.003	0.001	H→L (96%)	H-1→L (66%)	657.9	688.5
	1.950	1.744	0.002	0.003	H-2→L (61%)	H→L (95%)		
	2.013	1.873	0.001	0.002	H-1→L+1 (87%)	H-2→L (65%)		
3	2.494	2.497	0.031	0.034	H→L (85%)	H→L (84%)	489.0	489.0
	2.609	2.628	0.011	0.011	H→L+1 (96%)	H→L+1 (96%)		
	2.928	2.930	0.008	0.009	H-1→L+1 (79%)	H-1→L (76%)		
4	2.370	2.361	0.017	0.023	H→L (49%)	H→L (49%)	468.4	473.4
	2.645	2.618	0.033	0.046	H→L+2 (24%)	H→L (25%)		
	2.673	2.660	0.046	0.038	H-1→L (54%)	H-1→L (42%)		
5	2.094	2.078	0.028	0.023	H→L+2 (53%)	H→L+2 (43%)	489.0	500.0
	2.161	2.160	0.036	0.050	H→L+1 (52%)	H→L+1 (44%)		
	2.538	2.481	1.391	1.351	H-1→L (70%)	H-1→L (64%)		

^aIn eV.^bOnly major contribution to the transitions for each states are in parenthesis.^cH and L represent HOMO and LUMO, respectively.

Table 3 shows the results of time-dependent density functional theory (TDDFT) calculation including first 3 vertical excitation energy and its corresponding oscillator strength, orbital transition characters and maximum absorption wavelength (λ_{\max}) simulated in the 2 media. The first vertical excitations of **1** and **2** are approximately 1.8 eV in H₂O and ~1.7 - 1.8 eV in CH₂Cl₂ while the rest of them are about 2.1 - 2.5 eV in both media. HOMO→LUMO transition is the major transition (at the highest oscillator strength) for **2** and **3** in both 2 solvent phases and for **1** and **4** in CH₂Cl₂ media. Another transition such as H-1→L, H-2→L and H-1→L+1 play an important role for charge transition in the rest of the dyes. The simulated UV-Vis spectra of all dyes are shown in **Figure 4**. λ_{\max} of all dyes is ~10 - 20 nm red shifted from polar to non-polar media except for **1**. It is important to note that the use of non-polar solvent indicates the greatest significant effect on **1** while less significant is found on the other. Effect on the donor group is obviously dominated in **1** and **2** which their λ_{\max} is longer than those dyes **3,4** and **5**.

The isovalue plots of molecular orbitals of **1** and **2** are shown in **Figure 5** and of dyes **3 - 5** are shown in **Figure 6**, respectively. Based on **Figure 5**, electron density of HOMO and the 3 lower levels of **1** is located on the quinoxaline-2,3-dithiolate ligand showing the participation of Cu orbitals while the H-4 and H-5 distributed partly on bipyridine. Similar pattern is also found in **2**. This indicates that quinoxaline-2,3-dithiolate becomes a stronger donor unit than bipyridine for their corresponding photo excitation charge transfer. The metal to ligand charge transfer (MLCT) occurs in **1** and **2** is due to HOMO → LUMO transition as shown in **Table 3**. For **3**, electron densities of HOMO and H-1 are located on the acceptor unit (hydroxamate) instead of donor unit. H-2 is mainly located on the donor unit while it is spread out entire molecule in H-3 and H-5. Interestingly, densities of the virtual orbital are mostly distributed on hydroxamate. Thus, the HOMO→LUMO transition is not properly corresponded to the MLCT process. The excitations from H-2, H-3 and H-5 to all LUMO states seem to be related to MLCT than those of due to HOMO→LUMO even though it is assigned as main transition as shown in **Table 3**. In this case, excitation from H-2 to LUMO may be the major MLCT of **3** based on its smallest magnitude of vertical excitation energy compare to from other sub-energy levels; H-3, H-4 and H-5 to the LUMO state. Similarly, either HOMO→LUMO or H-1→L are assigned to be the major transition of **4** and **5**, but

in this case it is not MLCT process but just LLCT (ligand to ligand charge transfer) (**Figure 6**). The MLCT of **4** and **5** should be due to the excitation from the ground state HOMO to L+3 and L+2, respectively.

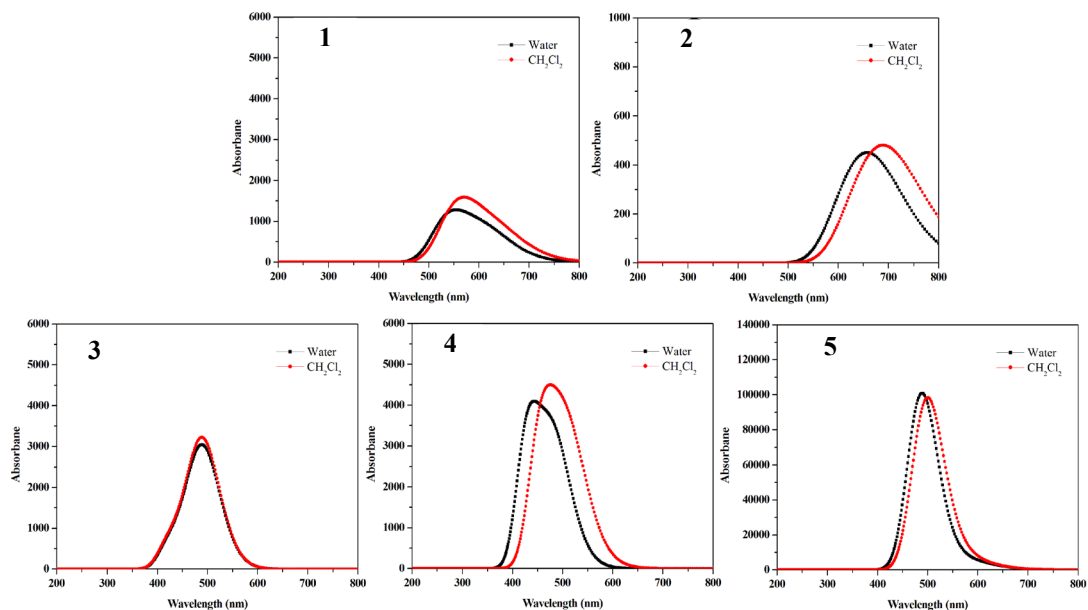


Figure 4 Isovalue plot of molecular orbital energies of dyes 1 and 2.

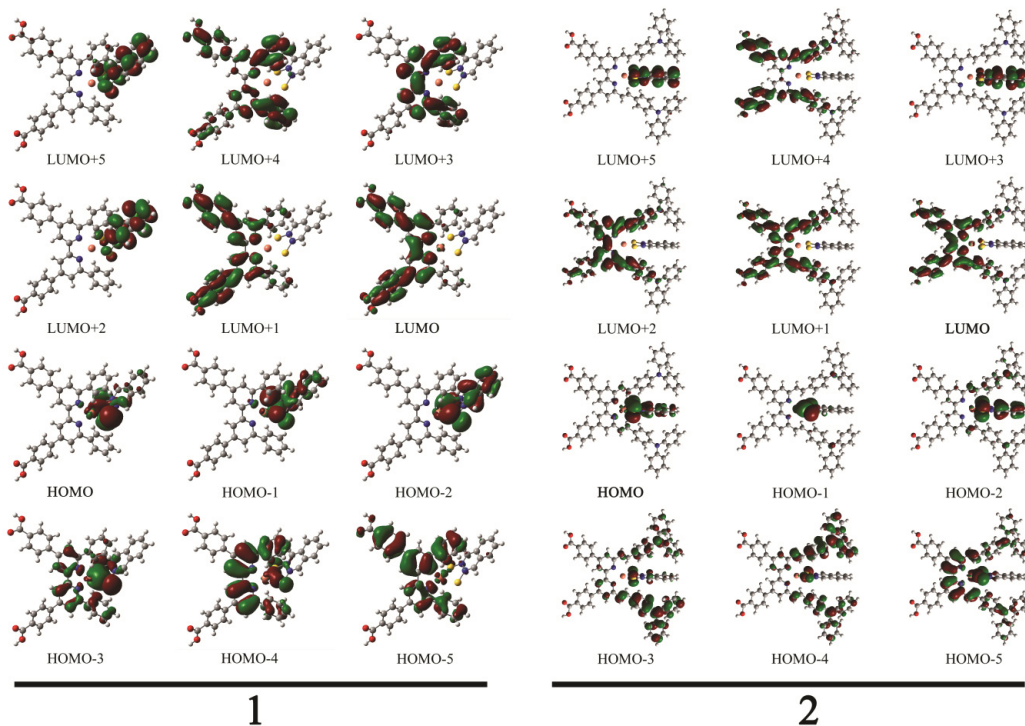


Figure 5 Isovalue plot of molecular orbital energies of dyes 1 and 2.

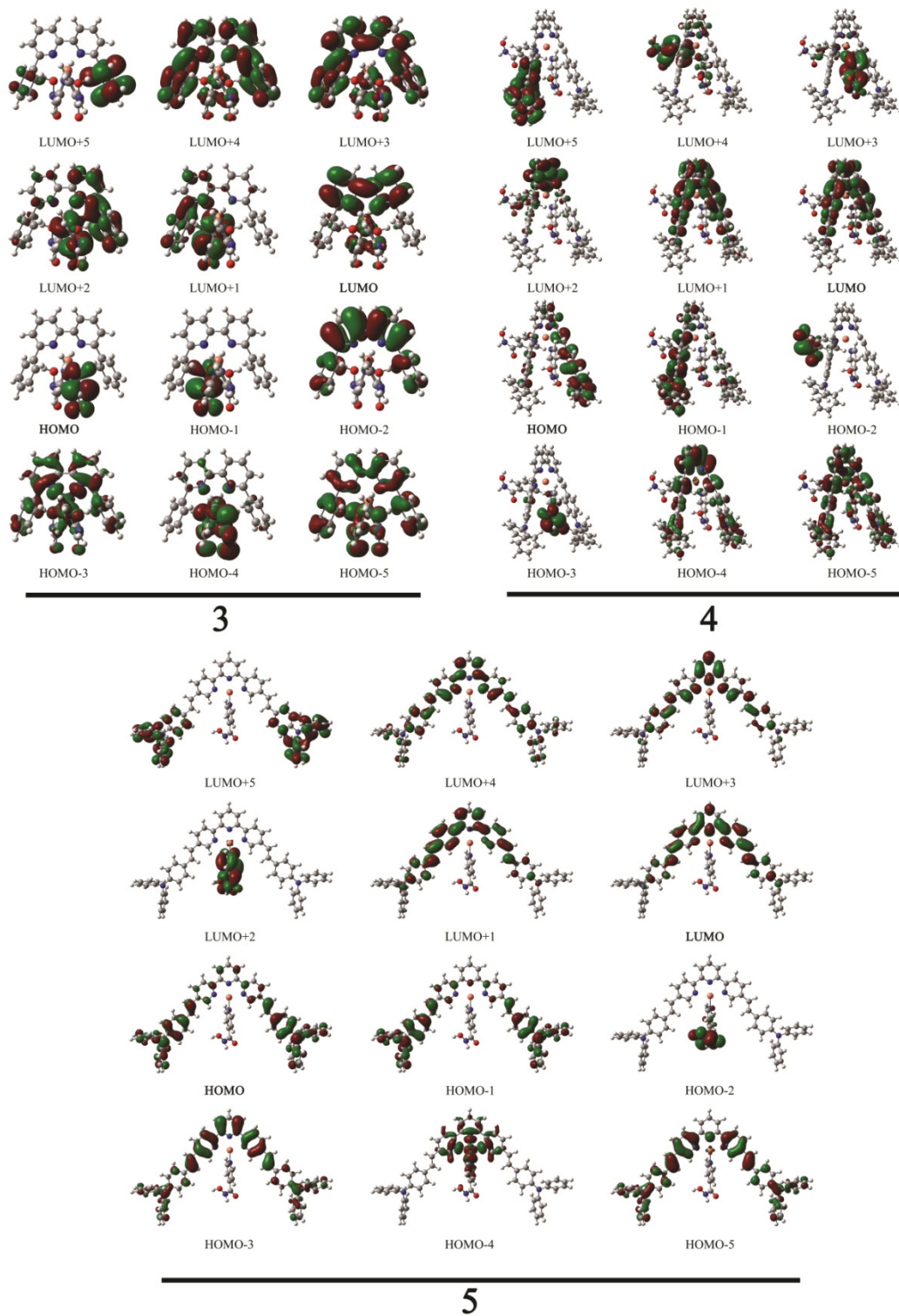


Figure 6 Isovalue plot of molecular orbital energies of dyes 3 - 5.

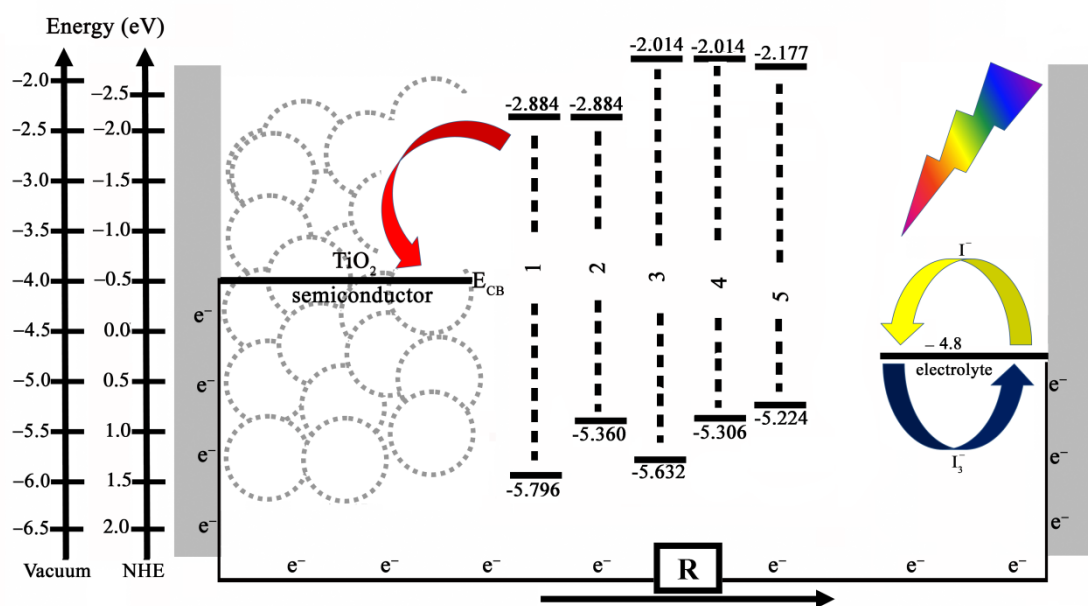


Figure 7 A schematic representation of MO energy levels of dyes relates to conduction band edge of TiO_2 and redox potential of I^-/I_3^- electrolyte.

The ground ($E_{\text{ox}}^{\text{dye}}$) and excited state ($E_{\text{ox}}^{\text{dye}^*}$) oxidation potentials, electron injection free energy (ΔG_{inject}), computed in the 2 solvent phases of all dyes are represented in **Table 4**. Ground state oxidation potential energy related to ionization potential energy can be estimated as negative E_{HOMO} [57]. The estimated value is in fair agreement with experimental values [62]. $E_{\text{ox}}^{\text{dye}^*}$ calculated due to Eq. (2) which the coulombic stabilization term is neglected [53]. $E_{\text{ox}}^{\text{dye}^*}$ of all dyes shows cathodic shift from polar to non-polar media. The most shift is found in **1** and **2** (~ 0.3 eV) while the lower shift is found in the rest (~ 0.2 eV). The cathodic shift indicates that the dyes possess lesser strength of oxidation while anodic shift indicates for more strength. According to $E_{\text{ox}}^{\text{dye}^*}$, it shows that the most oxidizing species is **4** in both polar and non-polar media. Dyes **1** and **2** are the worst oxidizing molecules in excited state. It is found that the strength of oxidation increases when Cu(I)bipyridine co-complexed with hydroxamate regards to quinoxaline-2,3-dithiolate ligand.

The electron injection free energy (ΔG_{inject}) computed based on Eq. (1) of all dyes are also presented in **Table 4**. All dyes possess spontaneous charge transfer indicates by negative value of ΔG_{inject} except for **1** in CH_2Cl_2 . Based on ΔG_{inject} , **4** as well as **5** are presented as highest and second highest performances among the others. The worst charge transfer ability is found in **1** and **2**. It is in accordance to the oxidation strength as described above. The LUMO- $E_{\text{CB}}^{\text{TiO}_2}$ gap corresponds to the estimated open circuit voltage as tabulated in **Table 5**. Thus, **3**, **4** and **5** will be possessed the highest, second highest and third highest performance of DSSC, respectively. A group of **1** and **2** are supposed to be the lowest performance. It should be noted that the concentration of dyes, pH and temperature have to be taken into account for consideration of experimental V_{OC} . Another aspect that has great influence on the performance of DSSC is light harvesting efficiency (*LHE*) of the dyes. The values are also shown in **Table 5**. Considering the term of *f* and its trend with *LHE* computed in non-polar media, it is clear that **3** is the most efficient, follow for **5** and **4**. As the same consideration, the trend of efficiency is in decreasing order: **3** > **5** > **1** > **4** > **7**. Thus, increasing chromophoric groups or conjugated bond does not favor to eV_{OC} and *LHE* in case of **4** and **5** regards to **3**.

Table 4 The ground state (E_{OX}^{dye}) and excited state (E_{OX}^{dye*}) oxidation potentials and free energy change for electron injection (ΔG_{inject}) of all dyes derived from orbital energy computed at the M06/LANL2DZ+DZVP of theory.

Dye	E_{OX}^{dye} ^a		E_{OX}^{dye*} ^a		ΔG_{inject} ^a	
	H ₂ O	CH ₂ Cl ₂	H ₂ O	CH ₂ Cl ₂	H ₂ O	CH ₂ Cl ₂
1	5.796	6.013	3.940	4.207	-0.060	0.207
2	5.360	5.551	3.528	3.872	-0.472	-0.128
3	5.632	5.877	3.139	3.380	-0.861	-0.620
4	5.306	5.469	2.936	3.108	-1.064	-0.892
5	5.224	5.442	3.131	3.364	-0.869	-0.636

^aIn eV.

Table 5 Estimated open-circuit voltage (eV_{oc}) and light harvesting efficiency (LHE) and of all dyes computed at the TD/M06/LANL2DZ+DZVP of theory.

Dye	eV_{oc} ^a		LHE ^b	
	H ₂ O	CH ₂ Cl ₂	H ₂ O	CH ₂ Cl ₂
1	1.116	0.844	0.047	0.047
2	1.116	0.844	0.007	0.003
3	1.986	1.742	0.068	0.075
4	1.959	1.714	0.038	0.050
5	1.823	1.606	0.062	0.052

^a In eV.

^b Computed based on the largest oscillating strength.

Thermodynamically, the spontaneous charge transfer process from the dye excited state to conduction band of TiO₂ requires higher level of LUMO than $E_{CB}^{TiO_2}$ (-4.0 eV) while HOMO energy level should be lower than reduction potential energy of the Γ/Γ_3 electrolyte (-4.80 eV) corresponds to the spontaneous charge regeneration. The schematic representation of energy level diagram of the HOMO and LUMO energy levels of the dyes and $E_{CB}^{TiO_2}$ and redox potential energy of the electrolyte simulated in H₂O is depicted in **Figure 7**. The LUMO levels of all dyes are above the $E_{CB}^{TiO_2}$ while their HOMO levels are lower than the redox potential energy of electrolyte. Thus, it can be noted that all of them possesses a positive response to charge transfer and regeneration related to photooxidation process. The largest gap between LUMOs of all dyes and $E_{CB}^{TiO_2}$ is found in **3** and **4** and the lowest gap is found in **1** and **2** corresponding to the highest and lowest charge transfer of the dyes. Similarly, the maximal gaps between redox potential of Γ/Γ_3 electrolyte and HOMO energy levels of dyes are found in **1** follow by **3**. It can be said that these dyes response highly to charge regeneration after their photooxidation process. On the other hand, **5** is assumed to response less charge regeneration due to its minimal HOMO- Γ/Γ_3 energy difference.

Conclusions

The optimized geometries, molecular orbitals electron density and their energy level, the parameters relates to photoelectrochemical properties of the 5 designed Cu(I) dyes were obtained from M06/LANL2DZ+DZVP method. For all complexes, molecular orbital energy levels meet the requirements for use as sensitizer in DSSC. Introducing the selected ligands has great effect to the MO energies as well as other properties. The quinoxaline-2,3-dithiolate (**1,2**) is great as donor unit. However, even the complexes **1** and **2** possess red shift in maximum absorption wavelength compared to the other but their electrophilic indices indicate that they have less strength of being oxidized. The results were supported by large magnitude of $E_{OX}^{dye^*}$ and less negative value ΔG_{inject} . Interestingly, hydroxamate ligand can be great potential acceptor unit for Cu(I) in bipyridine or terpyridine complexes (**3–5**). They also present good photochemical properties such as less magnitude of $E_{OX}^{dye^*}$ and high negative value of ΔG_{inject} . Thus, the designed dyes **3–5** studied in this work would be competent to provide promising sensitizers for photovoltaic application. **3** is the most promising among the other dyes. According to analyze these data, it is possible to find potential applications for these copper complexes in photovoltaic devices.

Acknowledgements

This work was financially supported by The National Research University Project, Khonkaen University and Office of Higher Education Commission through the research grant no. PD.57001 to WS was gratefully acknowledged. Faculty of Engineering, Rajamangala university of Technology Isan, Khonkaen campus and Institute of Research and Development, RMUTI were also acknowledged for partial support.

References

- [1] B O'Regan and M Grätzel. A low-cost, high-efficiency solar cell based on dye sensitized colloidal TiO₂ films. *Nature* 1991; **353**, 737-40.
- [2] A Hagfeldt, G Boschloo, L Sun, L Kloo and H Pettersso. Dye-sensitized solar cells. *Chem. Rev.* 2010; **110**, 6595-663.
- [3] I Repins, MA Contreras, B Egaas, C DeHart, J Scharf, CL Perkins, B To and R Noufi. 19.9%-efficient ZnO/CdS/CuInGaSe₂ solar cell with 81.2% fill factor. *Res. Appl.* 2008; **16**, 235-9.
- [4] X Wu. High-efficiency polycrystalline CdTe thin-film solar cells. *Sol. Energ.* 2004; **77**, 803-14.
- [5] M Wright and A Uddin. Organic-inorganic hybrid solar cells: A comparative review. *Sol. Energ. Mat. Sol.* 2012; **107**, 87-111.
- [6] YP Fu, ZB Lv, HW Wu, SC Hou, X Cai, D Wang and DC Zou. Dye-sensitized solar cell tube. *Sol. Energ. Mat. Sol.* 2012; **10**, 2212-9.
- [7] JB Asbury, RJ Ellingson, HN Gosh, S Ferrere, AJ Notzig and T Lian. Femtosecond IR study of excited-state relaxation and electron-injection dynamics of Ru(dcbpy)₂(NCS)₂ in solution and on nanocrystalline TiO₂ and Al₂O₃ thin films. *Phys. Chem. B* 1999; **10**, 33110-9.
- [8] NG Park, MG Kang, KM Kim, KS Ryu, SH Chang, DK Kim, J van de Lagemaat, KD Benkstein and AJ Frank. Morphological and photoelectrochemical characterization of core-shell nanoparticle films for dye-sensitized solar cells: Zn–O type shell on SnO₂ and TiO₂ cores. *Langmuir* 2004; **20**, 4246-53.
- [9] Y Saito, N Fukuri, R Senadeera, T Kitamura, Y Wada and S Yanagida. Solid state dye sensitized solar cells using in situ polymerized PEDOTs as hole conductor. *Electrochem. Commun.* 2004; **6**, 71-4.
- [10] C Jia, Z Wan, J Zhang, Z Li, X Yao and Y Shi. Theoretical study of carbazole-triphenylamine-based dyes for dye-sensitized solar cells. *Spec. Chim. Acta A* 2012; **86**, 387-91.
- [11] MJ Lee, KD Seo, HM Song, MS Kang, YK Eom, HS Kang and HK Kim. Novel D–π–A system based on zinc-porphyrin derivatives for highly efficient dye-sensitised solar cells. *Tetra. Lett.* 2011; **52**, 3879-82.

- [12] JK Lee and M Yang. Progress in light harvesting and charge injection of dye-sensitized solar cells. *Mat. Sci. Eng. B* 2011; **176**, 1142-60.
- [13] MK Nazeeruddin, E Baranoff and M Grätzel. Dye-sensitized solar cells: A brief overview. *Sol. Energ.* 2011; **85**, 1172-8.
- [14] N Robertson. Cu^I versus Ru^{II}: Dye-sensitized solar cells and beyond. *Chem. Sus. Chem.* 2008; **1**, 977-9.
- [15] AH Rendondo, EC Constable and CE Housecroft. Towards sustainable dyes for dye-sensitized solar cells. *Chimia* 2009; **63**, 205-7.
- [16] N Alonso-Vante, J Nierengarten and JP Sauvage. Spectral sensitization of large-band-gap semiconductors (thin films and ceramics) by a carboxylated bis(1,10-phenanthroline)copper(I) complex. *J. Chem. Soc. Dalton Trans.* 1994; **11**, 1649-54.
- [17] J Deng, Q Xiu, L Guo, L Zhang, G Wen and C Zhong. Branched chain polymeric metal complexes containing Co(II) or Ni(II) complexes with a donor-acceptor architecture: Synthesis, characterization, and photovoltaic applications. *J. Mater. Sci.* 2012; **47**, 3383-90.
- [18] T Bessho, EC Constable, M Grätzel, AH Redondo, CE Housecroft, W Kylberg, MK Nazeeruddin, M Neuburger and S Schaffner. An element of surprise-efficient copper-functionalized dye-sensitized solar cells. *Chem. Commun.* 2008; **32**, 3717-9.
- [19] EC Constable, AH Redondo, CE Housecroft, M Neuburger and S Schaffner. Copper(I) complexes of 6,6'-disubstituted 2,2'-bipyridine dicarboxylic acids: New complexes for incorporation into copper-based dye sensitized solar cells (DSCs). *Dalton Trans.* 2009; **33**, 6634-44.
- [20] CL Linfoot, P Richardson, TE Hewat, O Moudam, MM Forde, A Collins, F White and N Robertson. Substituted [Cu(I)(POP)(bipyridyl)] and related complexes: Synthesis, structure, properties and applications to dye-sensitized solar cells. *Dalton Trans.* 2010; **39**, 8945-56.
- [21] XQ Lu, SX Wei, CML Wu, SR Li and WY Guo. Can polypyridyl Cu(I)-based complexes provide promising sensitizers for dye-sensitized solar cells? A theoretical insight into Cu(I) versus Ru(II) sensitizers. *Phys. Chem. C* 2011; **115**, 3753-61.
- [22] B Bozic-Weber, EC Constable, CE Housecroft, M Neuburger and JR Price. Sticky complexes: Carboxylic acid-functionalized *N*-phenylpyridin-2-ylmethanimine ligands as anchoring domains for copper and ruthenium dye-sensitized solar cells. *Dalton Trans.* 2010; **39**, 3585-94.
- [23] M Sandroni, M Kayanuma, A Planchat, N Szuwarski, E Blart, Y Pellegrin, C Daniel, M Boujtita and F Odobel. First application of the HETPHEN concept to new heteroleptic bis(diimine) copper(I) complexes as sensitizers in dye sensitized solar cells. *Dalton Trans.* 2013; **42**, 10818-27.
- [24] B Bozic-Weber, EC Constable, SO Furer, CE Housecroft, LJ Troxler and JA Zampese. Copper(I) dye-sensitized solar cells with [Co(bpy)₃]^{2+/3+} electrolyte. *Chem. Commun.* 2013; **49**, 7222-4.
- [25] LN Ashbrook and CM Elliott. Correction to dye sensitized solar cell studies of a donor-appended bis(2,9-dimethyl-1,10-phenanthroline) Cu(I) dye paired with a cobalt-based mediator. *Phys. Chem. C* 2013; **117**, 3853-64.
- [26] J Huang, O Buyukcakir, MW Mara, A Coskun, NM Dimitrijevic, G Barin, O Kokhan, AB Stickrath, R Ruppert, DM Tiede, JF Stoddart, JP Sauvage and LX Chen. Highly efficient ultrafast electron injection from the singlet MLCT excited state of Cu(I)-diimine complexes to TiO₂ nanoparticles. *Angew. Chem. Int. Ed.* 2012; **51**, 12711-5.
- [27] A Colombo, C Dragonetti, D Roberto, A Valore, P Biagini and F Melchiorre. A simple copper(I) complex and its application in efficient dye sensitized solar cells. *Inorg. Chim. Acta* 2013; **407**, 204-9.
- [28] KA Wills, HJ Mandujano-Ramírez, G Merino, D Mattia, T Hewat, N Robertson, G Oskam, MD Jones, SE Lewis and PJ Cameron. Investigation of a copper(I) biquinoline complex for application in dye-sensitized solar cells. *RSC Adv.* 2013; **3**, 23361-9.
- [29] B Bozic-Weber, SY Brauchli, EC Constable, SO Furer, CE Housecroft and IA Wright. Hole-transport functionalized copper(I) dye sensitized solar cells. *Phys. Chem. Chem. Phys.* 2013; **15**, 4500-4.

- [30] B Bozic-Weber, V Chaurin, EC Constable, CE Housecroft, M Meuwly, M Neuburger, JA Rudd, E Schoenhofer and L Siegfried. Exploring copper(I)-based dye-sensitized solar cells: A complementary experimental and TD-DFT investigation. *Dalton Trans.* 2012; **41**, 14157-69.
- [31] B Bozic-Weber, EC Constable, CE Housecroft, P Kopecky, M Neuburger and JA Zampese. The intramolecular aryl embrace: From light emission to light absorption. *Dalton Trans.* 2011; **40**, 12584-94.
- [32] KA Wills, HJ Mandujano-Ramírez, G Merino, G Oskam, P Cowper, MD Jones, PJ Cameron and SE Lewis. What difference does a thiophene make? Evaluation of a 4,4'-bis(thiophene) functionalised 2,2'-bipyridyl copper(I) complex in a dye-sensitized solar cell. *Dyes Pigment.* 2016, **134**, 419-26.
- [33] J Cong, D Kinschel, Q Daniel, M Safdari, E Gabriellson, H Chen, PH Svensson, L Sun and L Kloof. Bis(1,1-bis(2-pyridyl)ethane) copper(I/II) as an efficient redox couple for liquid dye-sensitized solar cells. *J. Mater. Chem. A* 2016, **4**, 14550-5.
- [34] J Baldenebro-Lopez, N Flores-Holguina, J Castorena-Gonzalez and D Glossman-Mitnik. Molecular design of copper complexes as sensitizers for efficient dye-sensitized solar cells. *Photochem. Photobiol. A* 2013, **267**, 1-5.
- [35] J Baldenebro-López, J Castorena-González, N Flores-Holguín, J Almaral-Sánchez, D Glossman-Mitnik. Computational molecular nanoscience study of the properties of copper complexes for dye-sensitized solar cells. *Int. J. Mol. Sci.* 2012; **13**, 16005-19.
- [36] J Baldenebro-López, J Castorena-González, N Flores-Holguín, J Almaral-Sánchez and D Glossman-Mitnik. Theoretical study of copper complexes: Molecular structure, properties, and its application to solar cells. *Int. J. Photoenerg.* 2013; **2013**, 613064.
- [37] N Sekar and VY Gehlot. Metal complex dyes for dye-sensitized solar cells: Recent developments. *Resonance* 2010; **15**, 819-31.
- [38] A Islam, H Sugihara, K Hara, LP Singh, R Katoh, M Yanagida, Y Takahashi, S Murata and H Arakawa. New platinum(II) polypyridyl photosensitizers for TiO₂ solar cells. *New J. Chem.* 2000; **24**, 343-5.
- [39] TP Brewster, SJ Konezny, SW Sheehan, LA Martini, CA Schmuttenmaer, VS Batista and RH Crabtree. Hydroxamate anchors for improved photoconversion in dye-sensitized solar cells. *Inorg. Chem.* 2013; **52**, 6752-64.
- [40] MJ Frisch, GW Trucks, HB Schlegel, GE Scuseria, MA Robb, JR Cheeseman, G Scalmani, V Barone, B Mennucci, GA Petersson, H Nakatsuji, M Caricato, X Li, HP Hratchian, AF Izmaylov, J Bloino, G Zheng, JL Sonnenberg, M Hada, M Ehara, K Toyota, R Fukuda, J Hasegawa, M Ishida, T Nakajima, Y Honda, O Kitao, H Nakai, T Vreven, JA Montgomery, JE Jr Peralta, F Ogliaro, M Bearpark, JJ Heyd, E Brothers, KN Kudin, VN Staroverov, R Kobayashi, J Normand, K Raghavachari, A Rendell, JC Burant, SS Iyengar, J Tomasi, M Cossi, N Rega, JM Millam, M Klene, JE Knox, JB Cross, V Bakken, C Adamo, J Jaramillo, R Gomperts, RE Stratmann, O Yazyev, AJ Austin, R Cammi, C Pomelli, JW Ochterski, RL Martin, K Morokuma, VG Zakrzewski, GA Voth, P Salvador, JJ Dannenberg, S Dapprich, AD Daniels, Ö Farkas, JB Foresman, JV Ortiz, J Cioslowski and DJ Fox. *Gaussian 09 Revision A.1.* Gaussian, Wallingford, CT, 2009.
- [41] P Hohenberg and W Kohn. Inhomogeneous electron gas. *Phys. Rev.* 1964; **136**, B864-B871.
- [42] C Sosa, J Andzelm, BC Elkin, E Wimmer, KD Dobbs and DA Dixon. A local density functional study of the structure and vibrational frequencies of molecular transition-metal compounds. *Phys. Chem.* 1992; **96**, 6630-6.
- [43] Y Zhao and D Truhlar. The M06 suite of density functionals for main group thermochemistry, thermochemical kinetics, noncovalent interactions, excited states, and transition elements: Two new functionals and systematic testing of four M06-class functionals and 12 other functional. *Theo. Chem. Accounts* 2008; **120**, 215-41.
- [44] W Kohn and LJ Sham. Self-consistent equations including exchange and correlation effects. *Phys. Rev.* 1965; **140**, A1133-A1138.
- [45] R Parr and W Yang. *Density-Functional Theory of Atoms and Molecules.* Oxford University Press, New York, 1994.
- [46] HF Schaefer. *Methods of Electronic Structure Theory.* Plenum Press, New York, 1977.

- [47] J Tomasi, B Mennucci and R Cammi. Quantum mechanical continuum solvation models. *Chem. Rev.* 2005; **105**, 2999-3094.
- [48] W Sang-aroon, S Saekow and V Amornkitbamrung. Density functional theory study on the electronic structure of monascus dyes as photosensitizer for dye-sensitized solar cells. *Photochem. Photobiol. A* 2012; **236**, 35-40.
- [49] W Sang-aroon, S Laopha, P Chaiamornnugool, S Tontapha, S Saekow and V Amornkitbamrung. DFT and TDDFT study on the electronic structure and photoelectrochemical properties of dyes derived from cochineal and lac insects as photosensitizer for dye-sensitized solar cells. *J. Mol. Model.* 2013; **19**, 1407-15.
- [50] R Katoh, A Furube, T Yoshihara, K Hara, G Fujihashi, S Takano, S Murata, H Arakawa and M Tachiya. Efficiencies of electron injection from excited N3 dye into nanocrystalline semiconductor (ZrO_2 , TiO_2 , ZnO , Nb_2O_5 , SnO_2 , In_2O_3) films. *Phys. Chem. B* 2004; **108**, 4818-22.
- [51] D Rehm and A Weller. Kinetics of fluorescence quenching by electron and H-atom transfer. *Isr. J. Chem.* 1970; **8**, 259-71.
- [52] JL Goodman and KS Peters. Effect of solvent and salts on ion pair energies in the photoreduction of benzophenone by DABCO. *J. Am. Chem. Soc.* 1986; **108**, 1700-1.
- [53] JB Asbery, YQ Wang, E Hao, H Ghosh and T Lian. Evidences of hot excited state electron injection from sensitizer molecules to TiO_2 nanocrystalline thin films. *Res. Chem. Intermed.* 2001; **27**, 393-406.
- [54] A Hagfeldt and M Grätzel. Light-induced redox reactions in nanocrystalline systems. *Chem. Rev.* 1995; **95**, 49-68.
- [55] D Cahen, G Hodes, M Grätzel, JF Guillermeles and IJ Riess. Nature of photovoltaic action in dye-sensitized solar cells. *Phys. Chem. B* 2000; **104**, 2053-9.
- [56] T Koopmans. Über die zuordnung von wellenfunktionen und eigenwerten zu den einzelnen elektronen eines atoms. *Physica* 1933; **1**, 104-13.
- [57] S Xu, J Wang, F Zhao, H Xia and Y Wang. Photophysical properties of copper(I) complexes containing pyrazine-fused phenanthroline ligands: A joint experimental and theoretical investigation. *J. Mol. Model.* 2015; **21**, 313-23.
- [58] A Irfan and AG Al-Sehemi. Quantum chemical study in the direction to design efficient donor-bridge-acceptor triphenylamine sensitizers with improved electron injection. *J. Mol. Model.* 2012; **18**, 4893-900.
- [59] X Lu, CML Wu, S Wei and W Guo. DFT/TD-DFT investigation of electronic structures and spectra properties of Cu-based dye sensitizers. *J. Phys. Chem. A* 2010; **114**, 1178-84.
- [60] F De Angelis, S Fantacci and A Sgamellotti. An integrated computational tool for the study of the optical properties of nanoscale devices: Application to solar cells and molecular wires. *Theor. Chem. Accounts* 2007; **117**, 1093-104.
- [61] YX Weng, YQ Wang, JB Asbury, HN Ghosh and T Lian. Back electron transfer from TiO_2 nanoparticles to $FeIII(CN)_6^{3-}$: Origin of non-single-exponential and particle size independent dynamics. *J. Phys. Chem. B* 1999; **104**, 93-104.
- [62] SK Sharma, AI Inamdar, H Im, BG Kim and PS Patil. Morphology dependent dye-sensitized solar cell properties of nanocrystalline zinc oxide thin films. *J. Alloy. Compd.* 2011; **509**, 2127-31.